



A Power Load Rejection Test Measured Stress Analysis

Shaojia Yang^{1*}

¹ PowerChina Huadong Engineering Corporation Limited, Hangzhou, 311122, China

Corresponding author email: yang_sj1@hdec.com

Abstract. Hydropower station load rejection test measured data may be due to various reasons such as measurement methods, there is a big interference and how to manage the decomposition, the measured stress analysis calculation error, pressure pulsation, also there is a big difficulty. Measurement data of a hydropower station load rejection VMD decomposition, and the analysis of frequency on the decomposition, and calculate the amount of decomposition and the Pearson coefficient of the measured data, analysis of the correlation, combined to determine the noise, pressure pulsation, and the average pressure, provides the basis for the analysis of load rejection test inversion of hydropower stations.

Keywords: Vmd; Load shedding; Hydropower station

1 Introduction

A power station's water system is 3294.7 m, including water diversion system total length of 2846.6 m, total length of about 448.1 m tail water system. Turbine rated power output of 305.2 MW, rated head of 330 m, rated flow of 104.3 m³/s. Facade adopts "two-stage inclined" diversion system arrangement, flat in the central slope Settings section. Tail water system facade adopts "flat + inclined hole" way.

In this paper, based on the unit load rejection test at the plant site, analysis of the measured data and the results of numerical calculation, get the average pressure, test and verify the reliability of calculation, get revised the calculation error and the pressure pulsation, calculation and analysis was carried out on the extreme working condition of control, predict extreme value.

2 The Theory

VMD decomposition approach is to use an iterative search optimal solution of variational model to determine the weight of each decomposition of center frequency and bandwidth, are completely non-recursive model, the model for a collection of modal components and their respective center frequency, and each mode is smooth, after demodulation into baseband Konstantin Dragomiretskiy through the experimental results show that: for sampling and noise, this method is more robust [1-4].

© The Author(s) 2023

Z. Ahmad et al. (eds.), *Proceedings of the 2023 5th International Conference on Structural Seismic and Civil Engineering Research (ICSSCER 2023)*, Atlantis Highlights in Engineering 24,
https://doi.org/10.2991/978-94-6463-312-2_21

Assumes that the original signal is decomposed into k f a component, to ensure that the decomposition sequence for a center frequency limited bandwidth of the modal component, at the same time to estimate the bandwidth of each mode and minimizing the sum of the constraint to equal the sum of all the modal and the original signal, the VMD constraint variational model is as follows:

$$\min_{\{\mu_k, \omega_k\}} \left\{ \sum_k \left\| \partial_t \left[\left(\delta(t) + \frac{j}{\pi} \right) \times \mu_k(t) \right] e^{-j\omega_k t} \right\|_2^2 \right\}$$

$$s.t. \sum_k \mu_k = f \tag{1}$$

Where, the $\delta(t)$ as the Dirac distribution; $\mu_k(t)$ for the first k intrinsic mode functions; j for the plural unit; ω_k for the first k IMF center frequency; f the initial signal.

The introduction of quadratic penalty factor and Langrange multiplication operator variational constraint model is converted into unconstrained problems, there are:

$$L(\{\mu_k\}, \{\omega_k\}, \lambda) = \alpha \sum_{k=1}^k \left\| \partial_t \left[\left(\delta(t) + \frac{j}{\pi} \right) \times \mu_k(t) \right] e^{-j\omega_k t} \right\|_2^2 + \left\| f - \sum_{k=1}^k \mu_k(t) \right\|_2^2 + \left\langle \lambda(t), f(t) - \sum_{k=1}^k \mu_k(t) \right\rangle \tag{2}$$

Where, α for secondary penalty factor; $\lambda(t)$ for Langrange multiplication operator.

Pearson correlation coefficient R , the coefficient can be intuitive show each IMF component after signal decomposition with the correlation degree between the original signal, and then judge whether the IMF component needs to be filtered, its value is close to zero, shows that the correlation between them.

$$R(\text{imf}_i(t), X(t)) = \frac{\text{cov}(\text{imf}_i(t), X(t))}{\sigma_{\text{imf}_i(t)} \sigma_X(t)} \tag{3}$$

Where, for the IMF component and the covariance between the original signal; σ for standard deviation.

3 Data Analysis

This article mainly aims at pressure have the greatest relative difference of 3, 4 # machine double 100% load rejection test condition analysis, by VMD method of spiral case and draft tube measured pressure decomposition. Get the IMF components and by fast Fourier transform (FFT) to obtain the corresponding spectrum is shown in figure 1 ~ 4.

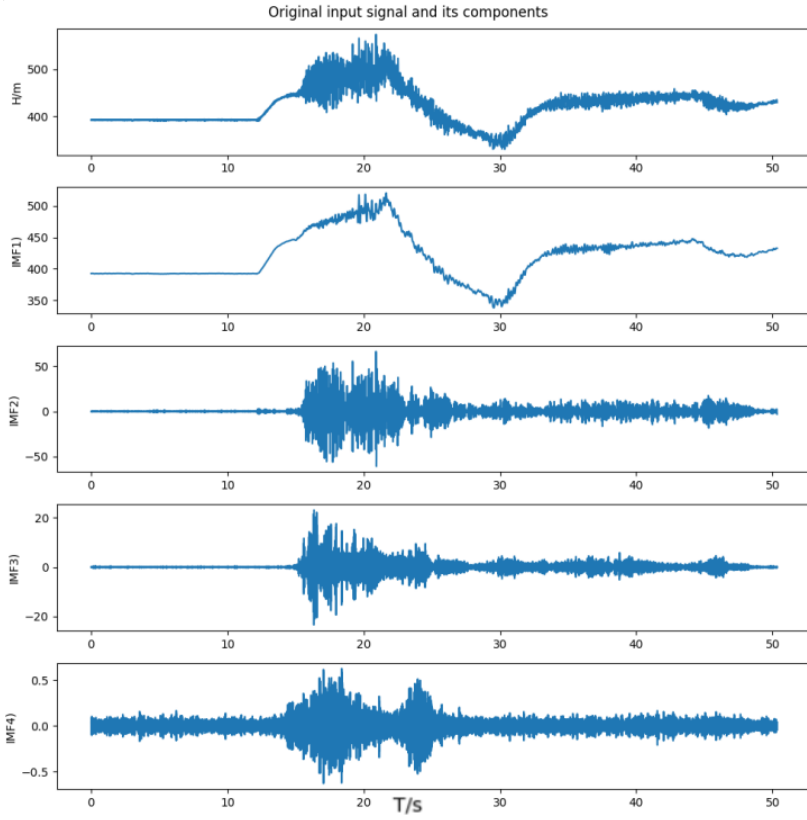


Fig. 1. Decomposition of VMD volute pressure

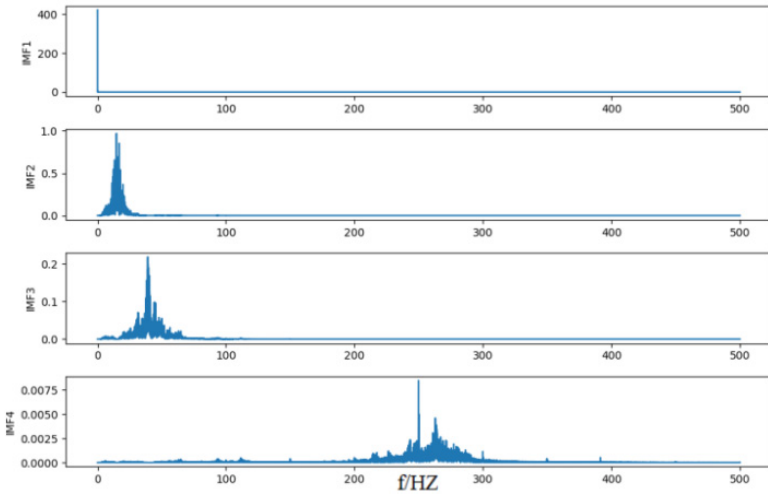


Fig. 2. Volute pressure spectrum

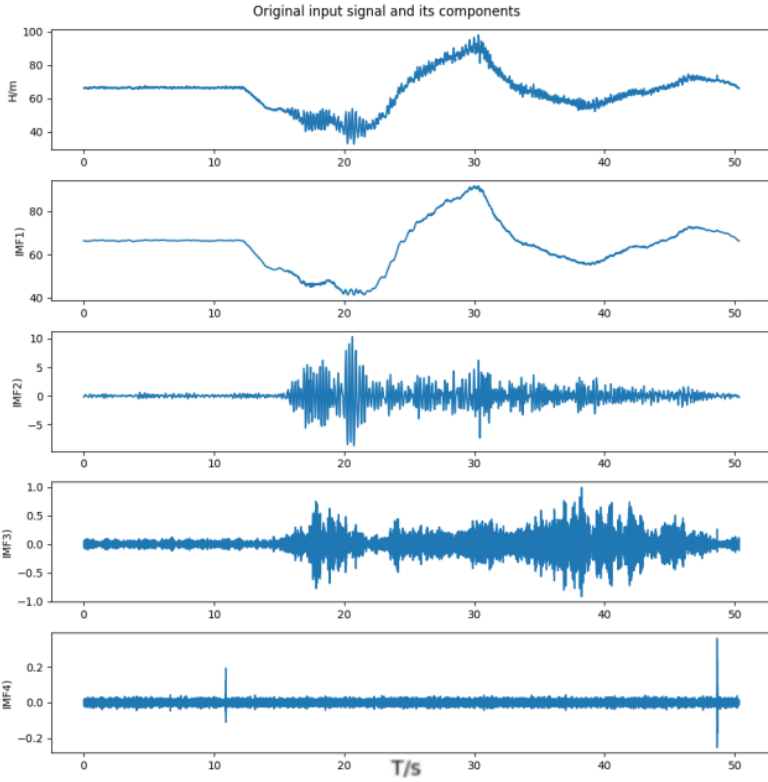


Fig. 3. Decomposition of VMD volute pressure

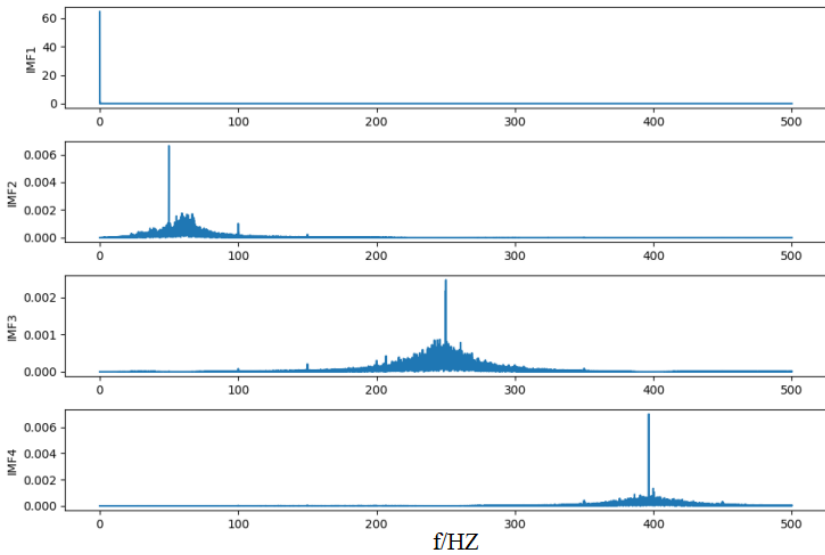


Fig. 4. Volute pressure spectrum

Volute pressure of center frequency decomposed each IMF component is respectively: 0 HZ, 15 HZ, 28 HZ and 260 HZ, Pearson correlation coefficient respectively: 0.97, 0.26, 0.08 and 0.01. Due to load rejection process, volute pressure pulsation in the main by high frequency noise interference (turn and instantaneous frequency multiple related) (generally not more than 20 HZ) and low frequency of rotating stall together, will be more than center frequency 50 HZ and the relationship between each other is below 0.1 component as the high frequency noise component of the IMF, the IMF as the pressure in the volute cross-section of the measured average, IMF2 and IMF3 as fluctuating pressure of the spiral case, the sum of IMF4 as high frequency noise component.

Draft tube inlet pressure of center frequency decomposed each IMF component is respectively: 0 HZ, 4 HZ, 60 HZ and 360 HZ, Pearson correlation coefficient respectively: 0.99, 0.15, 0.02 and 0.00. Due to load rejection process, within the draft tube pressure pulsation is given priority to with low frequency of vortex frequency band, so the imf as a draft tube measured average distribution in the cross section of the inlet pressure, the low frequency and the relationship with each other for higher import fluctuating pressure IMF2 component as the draft tube, IMF3 and IMF4 as high frequency noise component.

The pressure of the spiral case and draft tube inlet pressure contrast change process as shown in figure 5 ~ 6, extreme value contrast are shown in table 1. Maximum pressure of the spiral case calculation error to jilt before 3.82% of the net head, tail pipe entrance minimum pressure calculation error is left before the water head - 4.52%, therefore, the numerical simulation of high precision and can satisfy the precision requirement of power plant hydraulic transient process analysis. Simulated forecast extreme controlling conditions, can be obtained according to the calculation of error correction in table 1 mean water hammer pressure, according to the working condition of fluctuating pressure with proportional amplifier gain control of fluctuating pressure [5-7].

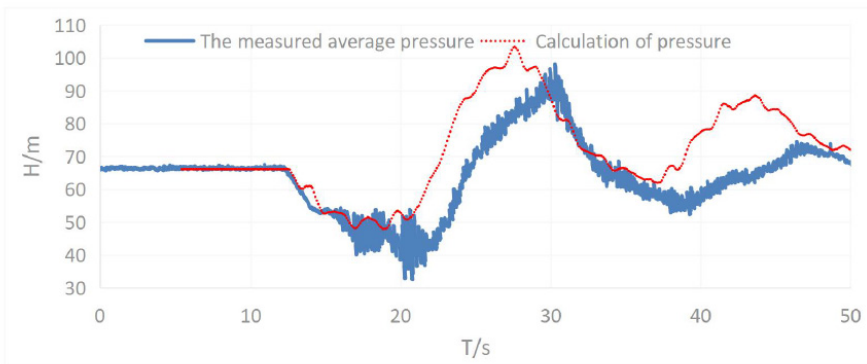


Fig. 5. volute pressure measured average compared with the simulation calculation value

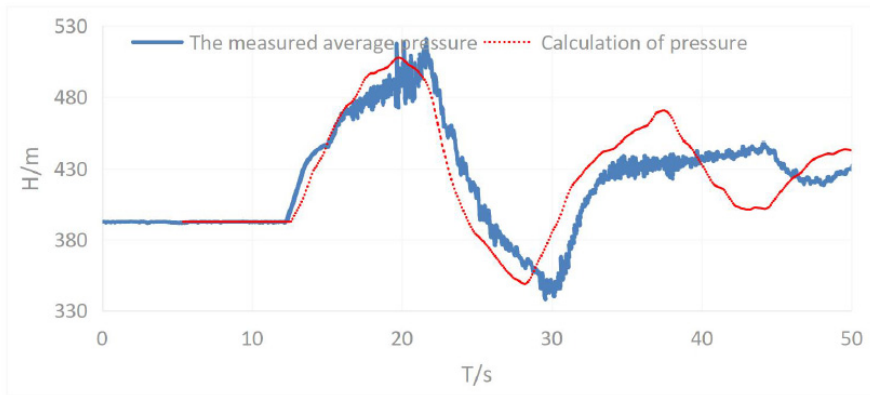


Fig. 6. draft tube inlet pressure measured average compared with the simulation calculation value

Table 1. the measured average extremum and simulate extreme contrast

| Control parameters | The measured average (m) | Calculated value (m) | Calculation error (%) | Pressure fluctuation (%) |
|---------------------------------------|--------------------------|----------------------|-----------------------|--------------------------|
| The import of maximum pressure | 520.75 | 507.81 | 3.82 | 20.15 |
| The tail pipe import minimum pressure | 32.63 | 47.95 | -4.52 | -2.57 |

Note: " $(\text{The measured average}-\text{Calculated value}) / \text{Net head before load rejection}$ " is adopted to define the calculation error, Pressure pulsation use " $\text{Fluctuating pressure} / \text{Net head before load rejection}$ ".

4 Conclusion

Based on the prototype of a hydropower station load rejection test measured data, this paper, by using VMD variational mode decomposition method of spiral case and draft tube inlet pressure measured in the time-frequency analysis, simulation of spiral case and draft tube imported pressure change process are in good agreement with those obtained in the VMD the decomposed the measured average, inverse modeling of high precision and can satisfy the requirement of the power station extreme controlling transition prediction precision, and provide the basis for safe and stable operation of the plant.

Reference

1. wei da, Wang Weiyu, Zhang Pei. Based on the nonlinear model of hydro turbine dynamic characteristic simulation [J]. Journal of hydropower station, mechanical and electrical technology, 2023, 46-48 (02): 12-17. DOI: 10.13599 / j.carol carroll nki. 11-5130.202302.004.

2. jian-qiang guo, Luo Guohu Wang Xi etc. Pumped storage unit load rejection test study [J]. Journal of hydropower station, mechanical and electrical technology, 2023, 46-48 (01): 12-15. DOI: 10.13599 / j.carol carroll nki. 11-5130.2023.01.004.
3. shi tao. Segmentation algorithm based on time domain of the circuit breaker fault vibration signal feature extraction method [J]. Electric power equipment management, 2021 (03): 158-159.
4. ZhangMengJie, li, Chen Nianhui etc. A hydropower station real machine test inversion calculation and in situ extreme condition prediction [J]. Water and electricity energy science, 2020, 20 (12): 153-155.
5. 'Mr. Rynning cao Jiang Lei, Chen Zhongbin etc. Based on the load rejection test of VMD tail pipe stress analysis and prediction [J]. China's rural water conservancy and hydropower, 2020 (02): 148-152.
6. the hui tung, Pan Luoping AnXueLi. VMD and permutation entropy based water turbine pressure pulsation signal denoising algorithm [J]. Journal of hydroelectric power, 2017, 4 (8): 78-85.
7. li will, Ding Jinghuan Yu Xuesong. Pumped storage units hydraulic interference test and prediction research [J]. Journal of dongfang review, 2015, 29 (01): 37-39. DOI: 10.13661 / j.carol carroll nki issn1001-9006.2015.01.009.

Open Access This chapter is licensed under the terms of the Creative Commons Attribution-NonCommercial 4.0 International License (<http://creativecommons.org/licenses/by-nc/4.0/>), which permits any noncommercial use, sharing, adaptation, distribution and reproduction in any medium or format, as long as you give appropriate credit to the original author(s) and the source, provide a link to the Creative Commons license and indicate if changes were made.

The images or other third party material in this chapter are included in the chapter's Creative Commons license, unless indicated otherwise in a credit line to the material. If material is not included in the chapter's Creative Commons license and your intended use is not permitted by statutory regulation or exceeds the permitted use, you will need to obtain permission directly from the copyright holder.

